Foam-based cleaning of surfaces contaminated with mixtures of oil and soot

Tamara Schad, Natalie Preisig, Wiebke Drenckhan, Cosima Stubenrauch

Received: 5 September 2021 | Revised: 10 December 2021 | Accepted: 27 December 2021

DOI: 10.1002/jsde.12580

ORIGINAL ARTICLE

AOCS WILEY

Foam-based cleaning of surfaces contaminated with mixtures of oil and soot

Tamara Schad[1] | **Natalie Preisig**[1] | **Wiebke Drenckhan**[2] | **Cosima Stubenrauch**[1,3]

[1]Institut für Physikalische Chemie, Universität Stuttgart, Stuttgart, Germany

[2]Université de Strasbourg, CNRS, ICS UPR 22, Strasbourg, France

[3]University of Strasbourg Institute for Advanced Studies (USIAS), University of Strasbourg, Strasbourg, France

Correspondence
Cosima Stubenrauch, Institut für Physikalische Chemie, Universität Stuttgart, Pfaffenwaldring 55, 70569 Stuttgart, Germany.
Email: cosima.stubenrauch@ipc.uni-stuttgart.de

Funding information
Deutsche Bundesstiftung Umwelt, Grant/Award Number: AZ 34788/01-45; H2020 European Research Council, Grant/Award Number: 819511-METAFOAM; University of Strasbourg Institute for Advanced Studies (USIAS)

Abstract

Liquid foams of intermediate stability have been shown to be very efficient in the cleaning of sensitive surfaces because of the synergy between imbibition and foam decay. While we quantified these mechanisms for contaminations with liquid oils in our previous work, we show here their extension to oils containing soot particles in an effort to simulate increasingly realistic contaminations. Using foams with a wide range of liquid fractions and with different stabilities, we show that the main cleaning mechanisms remain very similar, with the oil entraining the soot particles. However, we find much less efficient soot removal when the liquid channels of the foams are small enough to hinder efficient transport of the soot particles.

KEYWORDS
cleaning mechanisms, cleaning with foams, model contaminations (oil and soot)

INTRODUCTION

Historical surfaces of artistic and cultural assets are often soiled as a result of long-term exposure to different environmental processes, such as physical deposition, chemical degradation, and biogenic contamination, for example, from microbial activity. Typical examples of physically deposited compounds are grease (from touching the surfaces) and soot (from the atmosphere). In the long run, these pollutants can cause serious damage to the original surfaces and therefore have to be removed. Cleaning historical surfaces is quite difficult and time consuming. Each individual surface needs its own cleaning method in order not to harm the surface. Colloidal and materials sciences have made significant advances in the preservation of cultural assets over the past 20 years using various formulations and methods to clean historical surfaces (Baglioni et al., 2013). These include the use of new environmentally friendly, surfactant-based self-assembled systems, various types of emulsions, microemulsions, hydrogels and organogels, nanoparticle dispersions in apolar solvents, or hybrid organic–inorganic nanocomposite systems (Baglioni et al., 2013; Chelazzi et al., 2018). Our research is focused on developing a new foam-based cleaning method for sensitive surfaces in general and historical surfaces in particular (Schad et al., 2021). Foams are object-friendly alternatives to traditional cleaning solutions especially in cases where exposure to the cleaning solution needs to be limited. Furthermore, cleaning with foams is much more environmentally friendly, as the amount of surfactant can be reduced by more than 90% compared to the use of non-foamed cleaning solutions (Schad et al., 2021).

Recent research shows that foamed surfactant solutions can clean far more efficiently in comparison to their non-foamed counterparts (Andreev, Freer, et al., 2010; Andreev, Prausnitz, & Radke, 2010; Fournel et al., 2013; Jones et al., 2016; Schad et al., 2021), which

is due to foam-specific physical cleaning mechanisms. In our previous study (Schad et al., 2021), we were able to identify three cleaning mechanisms by performing cleaning tests with foams with different liquid fractions and different stabilities. We showed that because of the interplay among these three mechanisms, foams are a very good cleaning tool under certain conditions (Schad et al., 2021). The first mechanism is the ability of foams to suck in liquids due to capillary forces, which has been well established in the literature as "imbibition" (Mensire et al., 2015, 2016; Mensire & Lorenceau, 2017; Schad et al., 2021). Imbibition is most efficient in foams with low liquid fractions and small bubble sizes. The second mechanism is "wiping," that is, the foam bubbles perform wiping actions on the surface as a result of the movement of the contact line between dirt (oil), the solid surface, and the foam film (Schad et al., 2021). This wiping is driven by the inherent instability of liquid foams in which bubbles burst and move permanently. The third mechanism involves gravity-driven drainage of the cleaning solution in foams with high liquid fractions. The cleaning process is therefore dominated by different mechanisms whose efficiency depends on the bubble size and the liquid fraction. Imbibition and wiping are the dominant mechanisms at small bubble sizes and low liquid fractions, while the cleaning process is dominated by wiping and drainage at higher liquid fractions. We found that efficient wiping takes place only in sufficiently unstable foams (Schad et al., 2021) and that it plays a significant role in cleaning. For the cleaning of sensitive surfaces, we regard the foam-based cleaning process efficient if the following requirements are met: (i) significant drainage of the cleaning solution out of the foam can be prevented; (ii) the foam can accumulate different contaminants (such as oils, soot, etc.); and (iii) high cleaning sufficiency can be achieved in a short period. We showed that all these requirements are fulfilled by foams with low liquid fractions ($\varepsilon \leq 5\%$, e.g., the foam consists of 5 vol% liquid and 95 vol% gas), small bubble sizes, and limited stability (Schad et al., 2021).

The present study is a follow-up of our previous work (Schad et al., 2021), which we extend by using two — instead of one — model contaminations. We investigated the cleaning effect and the cleaning process of foams by using red-colored sunflower oil and soot particles as model contaminants. The cleaning foams were prepared using the double-syringe technique of Gaillard et al. (2017), as described in our previous study, with different liquid fractions but identical bubble sizes. The cleaning foams were applied to glass substrates contaminated with the two-component model contamination. As in our previous work (Schad et al., 2021), cleaning tests were carried out with foams whose gas phase either contained perfluorohexane (PFH) (stable foam) or did not contain PFH (unstable foam) to investigate the influence of foam stability on the cleaning process. We show and discuss whether the cleaning process with foams is impacted by the new model soiling and how the three different mechanisms, namely imbibition, wiping, and drainage, are involved in the cleaning process.

MATERIALS AND METHODS

Chemicals

The technical alkyl polyglycoside surfactant Glucopon 215 UP (C_nG_m with $n = 8$–10 and $m = 1.5$) was donated by BASF (Ludwigshafen, Germany) and used as received. Citric acid (99%, Aldrich, St. Louis, MO, USA), ammonia solution 25% (Merck, Darmstadt, Germany), the oil-soluble dye Sudan Red 7B (Kremer Pigmente, Aichstetten, Germany), and perfluorohexane (PFH) (99%, Aldrich) were used as purchased. Sunflower oil (brand name JA) was purchased from the supermarket (Rewe Group, Köln, Germany). Double-distilled water was used for the preparation of the aqueous cleaning solutions. The soot (carbon black [lamp black], amorphous) was purchased from Kremer Pigmente. The approximate diameter of the particles was between 15 and 300 nm (Long et al., 2013). However, the particles formed aggregates with a diameter of 85–500 nm, which in turn formed agglomerates with an approximate diameter ≥1 μm (Long et al., 2013). In our experiments with oil, the particles formed larger agglomerates with diameters between 30 and 160 μm.

Cleaning solutions

Aqueous solutions of Glucopon 215 UP with a concentration of 90 cmc (cmc = 0.89 g L^{-1}) were used for foam generation. The cmc was determined by surface tension measurements using the Du Noüy ring method and an STA1 tensiometer from Sinterface Technologies (Berlin, Germany; see Supporting Information in Schad et al., 2021). Since the aqueous Glucopon solutions have a pH of 11.5–12.5 — which can damage sensitive surfaces — the pH was buffered to a value of 8–8.5 by adding citric acid and ammonia solutions.

Model contaminated surfaces and experimental procedure

Circular glass plates with a diameter of 8 cm were used as model surfaces. The glass plates were cleaned with water and a lint-free tissue before each measurement. The contact angle of water on the glass plates is about $(30 \pm 4)^\circ$. We contaminated the cleaned glass plates with oil and soot. For this purpose, a 0.1-ml droplet of

colored sunflower oil (saturated with Sudan Red 7B) and a small amount of soot (covering the tip of a spatula) were applied to the middle of the glass plate, mixed, and spread over an area of approximately 9 mm^2 with a spatula (Figure 2a). The cleaning foams were generated with the double-syringe technique (see "Double-syringe technique" section) and placed on the contaminated glass plates immediately after generation (several minutes after applying the model contaminants to the glass plates). Note that the surfactant solution that drains from the foam flows from the glass plate to the outflows in the glass plate holder (Figure 2a). For analyzing the imbibition and drainage process, additional tests were carried out in a glass cuvette (28 ± 0.2 mm light path, $h = 35$ mm, $w = 35$ mm, $d = 32$ mm) with 1 ml of the colored sunflower oil and soot particles at the bottom. The foam was subsequently placed on top of the oil. In this case, the surfactant solution that drains from the foam was collected at the bottom of the cuvette.

Double-syringe technique

For the generation of foams with different liquid fractions, the double-syringe technique was used (Gaillard et al., 2017). The foam generation process is described in detail elsewhere (Schad et al., 2021). Briefly, to generate the foams two 60-ml syringes were connected with a Luer-Lock connector. One syringe was filled with a specific amount of the cleaning solution V_L and air V_G (in proportions corresponding to the liquid fraction $\varepsilon = V_L/[V_L + V_G]$) and connected to the second syringe, whose piston was in the fully closed position. The gas–liquid mixture was repeatedly pushed by hand (20 times) through the connector to generate the foam, which then homogeneously filled the whole syringe volume ($V_F = V_L + V_G$). For the generation of foams containing perfluorohexane (PFH) in the gas phase, a drop of PHF (which is liquid, but extremely volatile at room temperature with a vapor pressure of $p_{PFH} \approx 0.3$ bar at 25°C; Crowder et al., 1967) was placed on the piston of the second syringe before connecting to the first one. For the study at hand, foams with liquid fractions of $\varepsilon = 5\%$, 10%, 15%, and 20% were generated ($\varepsilon = 5\%$ was the lowest possible liquid fraction at which the gas was completely included into the foam in the syringe). Because of the formation of very small bubbles with an average radius of $\langle r \rangle = 60\,\mu m$ (Figure 1), a huge gas/solution interface is formed, which is why a high surfactant concentration ($c = 90$ cmc) is required to prevent depletion (Boos et al., 2012). The change of the mean bubble radius of the foam over time is shown in Figure 1 for the PFH-free (left) und PFH-containing (right) foam. While the bubble size of the stable PFH-containing foams remains nearly constant within 60 min, the mean radius of the bubbles of the unstable PFH-free foams increases by a factor of five within 30 min (Schad et al., 2021). Note that it was shown only recently that this important difference in foam stability results from the simultaneous suppression of foam coarsening and bubble coalescence by PFH (Steck et al., 2021).

Optical home-made setup for cleaning process study

A home-made optical setup (Figure 2) was used to monitor and analyze the cleaning process by measuring the area A_{dirt} covered by the contamination during the cleaning tests (see Schad et al., 2021 for more details). Briefly, the contaminated glass plate was fixed on top of the setup (Figure 2a). After placing foam on the contaminated glass plate, a digital camera was switched on, which recorded the cleaning process from

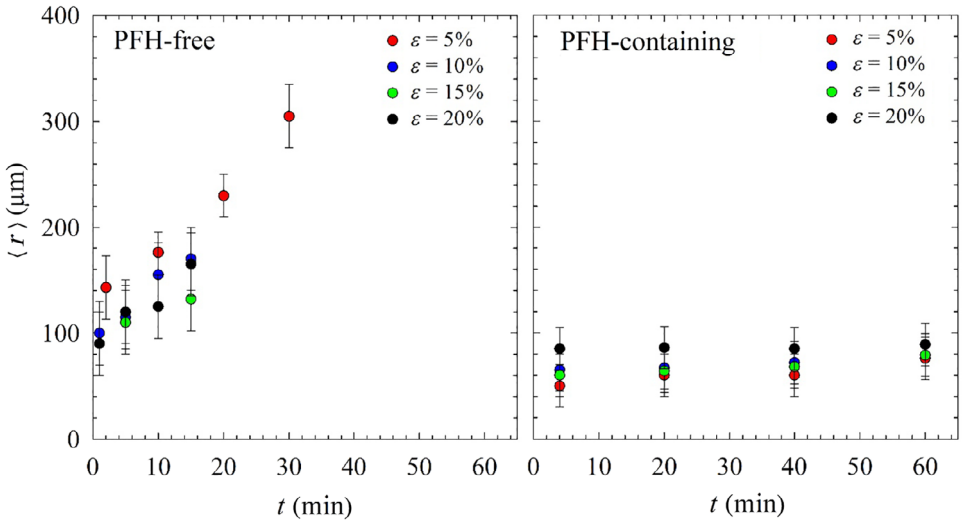

FIGURE 1 Mean bubble radius $\langle r \rangle$ as a function of time of foams with different liquid fractions ε without PFH (left) and with PFH (right) in the gas phase (reprinted from Schad et al., 2021 with permission from Elsevier)

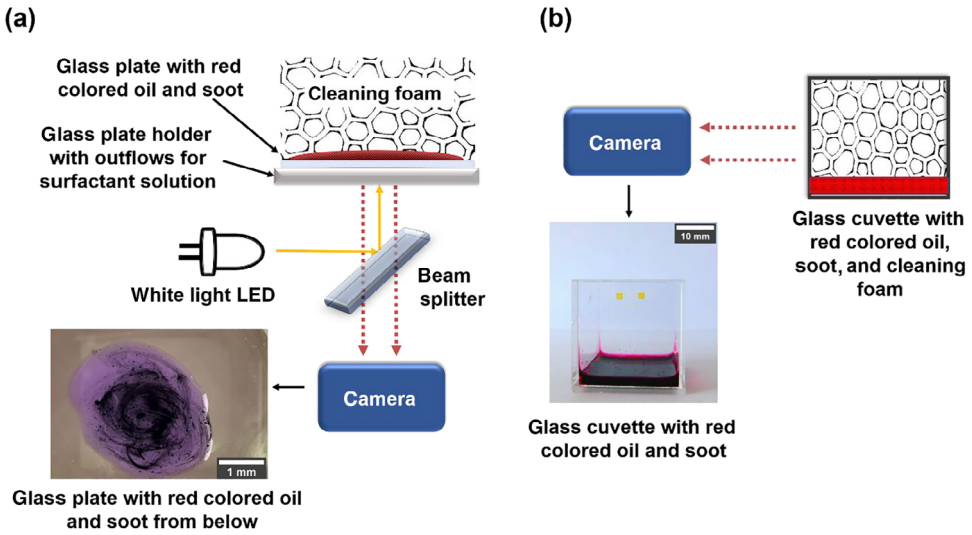

FIGURE 2 Experimental optical setup for studying (a) the cleaning process from the bottom (the surfactant solution that drains on the glass plate is removed by outflows in the glass plate holder) and (b) the imbibition and drainage from the side

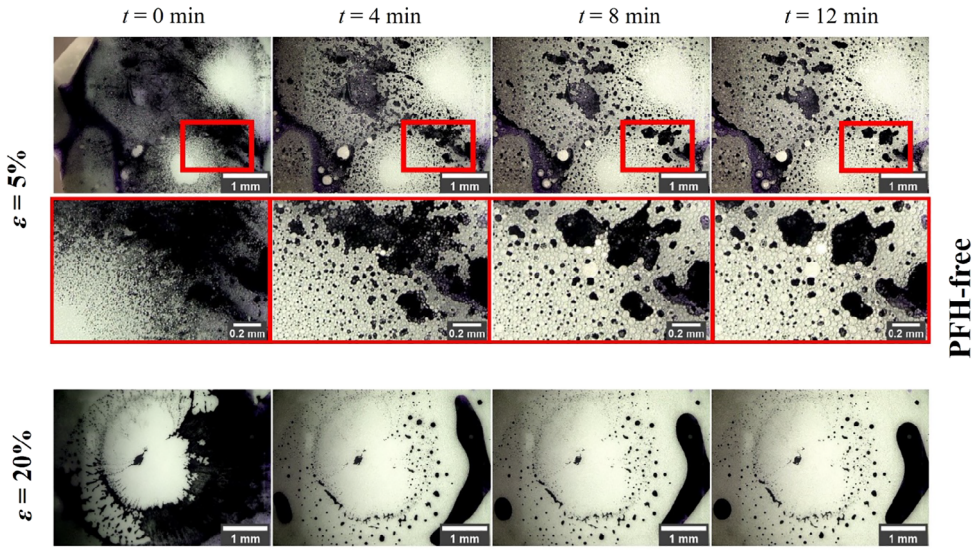

FIGURE 3 Photographs of the cleaning tests from the bottom with the PFH-free foams with $\varepsilon = 5\%$ and 20% right after the application and after 4, 8, and 12 min. The row of photographs (framed in red) in the middle shows a zoom into the red marked area of the images of the cleaning with $\varepsilon = 5\%$

the bottom. A white LED was used as the light source and a dichroic filter as a beam splitter. The camera software Toupsky and the commonly used program Fiji (ImageJ) (Schneider et al., 2012) were used to edit and analyze the pictures (see Figure S1). For observing the imbibition and drainage from the side, a glass cuvette with 1 ml oil and a small amount of soot (covering the tip of a spatula) at the bottom was filled up with the cleaning foam and placed in front of the camera. The processes taking place were recorded every minute with the digital camera manually (Figure 2b).

RESULTS AND DISCUSSION

General cleaning ability of PFH-free and PFH-containing foams

In this study, we performed cleaning experiments using foams with different liquid fractions ($\varepsilon = 5\%$, 10%, 15%, 20%) with and without PFH in the gas phase. We investigated how the cleaning process and cleaning efficiency are impacted by the liquid fraction and the foam stability and compared the results with the cleaning of glass plates contaminated with sunflower oil only. First, the PFH-free foams with different liquid fractions were deposited on the contaminated glass plates and the evolution of the contaminated area A_{dirt} (see "Optical home-made setup for cleaning process study" section and Figure S1) was investigated during the cleaning tests. Examples of typical images are shown in Figures 3 and 4. The same cleaning tests were repeated with very stable PFH-containing foams with the same liquid fractions. In these foams, coarsening and coalescence of the foam bubbles is efficiently prevented by the PFH (Andrieux et al., 2018; Gandolfo & Rosano, 1997; Höhler et al., 2008; Meagher et al., 2015; Schad et al., 2021; Steck et al., 2021; Weaire & Pageron, 1990), leading to a nearly constant bubble size during the experiment (Figure 1, right).

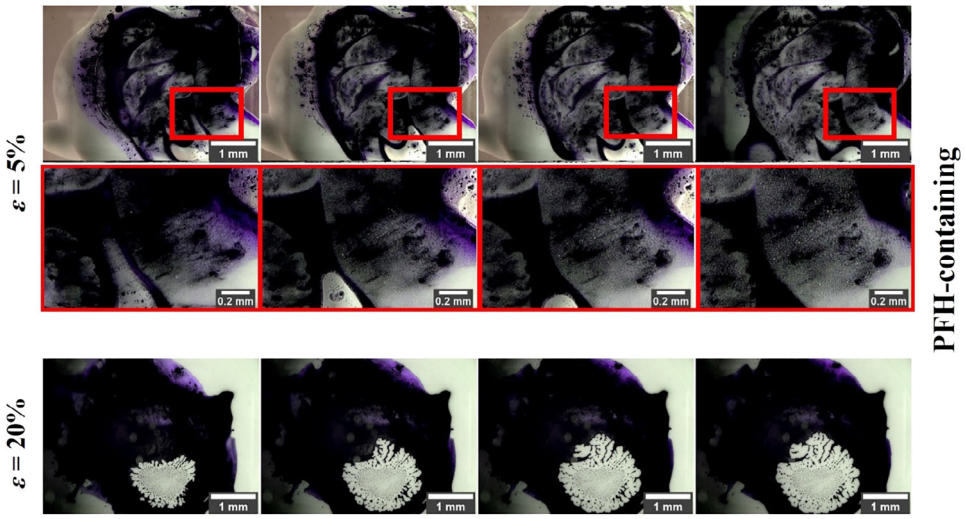

FIGURE 4 Photographs of the cleaning tests from the bottom with the PFH-containing foams with $\varepsilon = 5\%$ and 20% right after the application and after 4, 8, and 12 min. The row of photographs (framed in red) in the middle shows a zoom into the red marked area of the images of the cleaning with $\varepsilon = 5\%$

Photographs in Figure 3 show the first 12 min of cleaning with PFH-free foams. The contaminated surface covered with PFH-free foams with $\varepsilon = 5\%$ is shown in Figure 3 (top) and with $\varepsilon = 20\%$ in Figure 3 (bottom) at different times. The red framed row of photographs in the middle shows a zoom into the red marked area of the images of the cleaning with $\varepsilon = 5\%$. Photographs of cleaning tests with foams with liquid fractions of $\varepsilon = 10\%$ and $\varepsilon = 15\%$ are shown in Figure S2. The photographs at $t = 0$ min show the glass plate contaminated with soot (black) and colored sunflower oil (purple) from below directly after the application of the foam. The visible contaminated area on the glass plate is reduced in all cleaning tests with time. Looking at Figure 3 (top and middle), one sees that the contaminated area is split into many small areas with foam in between. The borders of the small areas are rather jagged like in our previous cleaning tests without soot (Schad et al., 2021). Moreover, part of the contamination disappears during cleaning, that is, the contaminants are sucked into the foam via capillary forces (mechanism I = imbibition) at low liquid fractions ($\varepsilon = 5\%$) (Schad et al., 2021). With increasing liquid content, one can see a change in the cleaning process from mechanism I (imbibition) to mechanism III (drainage). In Figure 3 (bottom), one sees that at $\varepsilon = 20\%$ the contaminated area is pushed together to form a big area with rounded edges during cleaning. In addition, a few smaller round droplets are formed. This is in line with the observations of our previous study and can be ascribed to mechanism III, that is, drainage. Here, the liquid drains out of the foam and forms a layer of water between the glass plate and the foam on which the contamination floats.

Photographs of the cleaning with PFH-containing foams during the first 12 min are shown in Figure 4. One can see the contaminated surface covered with PFH-containing foams with $\varepsilon = 5\%$ (Figure 4, top) and $\varepsilon = 20\%$ (Figure 4, bottom) at different times of the cleaning tests. Photographs of cleaning tests with the PFH-containing foams with liquid fractions of $\varepsilon = 10\%$ and $\varepsilon = 15\%$ are shown in Figure S3. Only a very small and very slow cleaning effect can be seen in all pictures. The contaminated area barely changes during the first 12 min of cleaning with the foam with $\varepsilon = 5\%$. When zooming into the photographs, one sees that some oil (purple) has disappeared during the cleaning. The oil was sucked into the foam (Schad et al., 2021). With the increase of the liquid fraction, the cleaning process changes from mechanism I (imbibition) to mechanism III (drainage) and is slightly more effective. One sees how the contaminated area is reduced in some places with foams with high liquid fractions ($\varepsilon \geq 10\%$). However, there is no separation of the contaminated area into small droplets as in our previous study without soot particles (Schad et al., 2021). In the present case, only the displacement of the dirt in the middle of the images of the tests with $\varepsilon = 15\%$ (Figure S3) and $\varepsilon = 20\%$ (Figure 4) is visible. Also, the edges of the dirt do not become rounder. Obviously, a smaller amount of liquid that drains from the PFH-containing foams is not enough to push the oil with the soot particles together (see "Imbibition and drainage viewed from the side" section).

One can observe significant differences by comparing the photographs of the cleaning with the unstable PFH-free (Figures 3 and S2) and the stable PFH-containing (Figures 4 and S3) foams. The unstable PFH-free foams show a good cleaning effect at all liquid contents. The stable PFH-containing foams show almost no cleaning effect even at higher liquid contents. The results of all cleaning tests with and without PFH are summarized in Figure 5. The plot shows the change of the contaminated area A_{dirt} on the glass plate as a function of time t for the PFH-free (Figure 5, left) and the PFH-containing (Figure 5, right) foam for each liquid fraction. We define the area of the contamination at $t = 0$ min as the reference area corresponding to

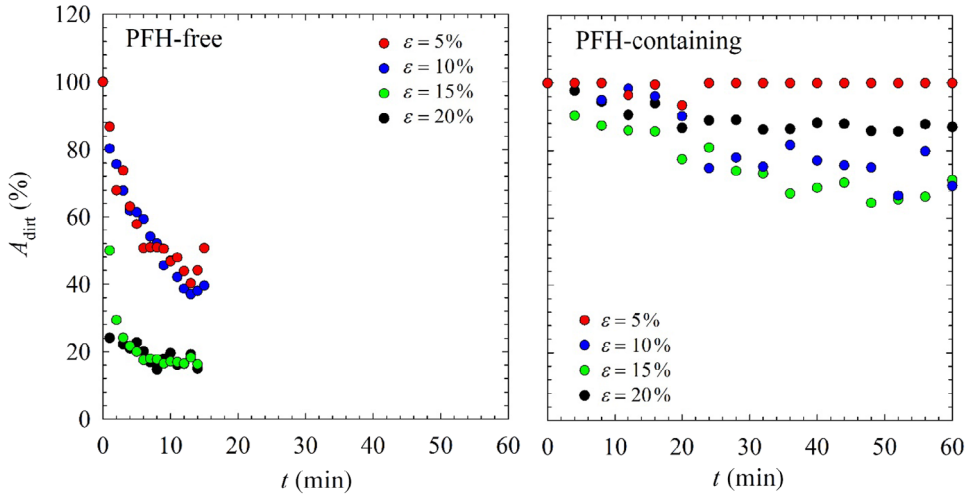

FIGURE 5 Time evolution of the contaminated area A_{dirt} (in percent) during the cleaning of the glass plates with PFH-free (left) and PFH-containing (right) foams of different liquid fractions

$A_{dirt} = 100\%$. The experiment time was set to 60 min for the PFH-containing foams because of the very slow cleaning process (Schad et al., 2021). The limit of 15 min was set for the PFH-free experiments because the PFH-free foam decays very quickly, as can be seen in Figure 1 (left), which shows that the bubble size doubles during the first 20 min. Moreover, the PFH-free foam starts to decay after a couple of minutes; after nearly 12 min, oil is "freed" as a result of the decay and hence flows back on the surface. Thus, it is important to take off the foam after a couple of minutes.

In Figure 5 (left), one can clearly see two different regimes in cleaning with unstable PFH-free foams. Depending on the liquid fraction, different cleaning mechanisms are involved in cleaning with foams. At low liquid fractions ($\varepsilon \leq 10\%$), imbibition takes place (mechanism I) in both foams with and without PFH in the gas phase. In this process, the liquid contamination (colored oil) is sucked into the foam (Mensire et al., 2015, 2016). The good cleaning effect of the unstable PFH-free foams indicates that the solid contamination (soot) can also be sucked into the foam. The soot particles are sucked into the foam together with the liquid dirt and detached from the surface by shear forces. These forces are caused by mechanism II. Wiping (mechanism II) takes place at all liquid fractions in unstable foams because of the permanent movement of foam bubbles during foam decay (Schad et al., 2021). During wiping, the surfactant molecules get adsorbed at both the oil and the soot surfaces, thus rendering the contaminates hydrophilic. Owing to the reduced adhesion between the glass plate and the contaminants, the latter can be sucked in by the foam via imbibition. This additional effect explains the better cleaning efficiency of the unstable PFH-free foams compared to stable PFH-containing foams at low liquid fractions (Figure 5). Imbibition also takes place in the case of stable foam, but there is no reduction in the contaminated area. It seems that in this case the particles cannot be drawn into the foam together with the oil. The lower cleaning efficiency of PFH-containing foams could be due to the smaller Plateau borders (see Section S3) of the foam and the lack of shear forces in the PFH-containing foams.

At higher liquid fractions ($\varepsilon \geq 15\%$), the cleaning process of the unstable and stable foams changes. If the liquid fraction is high enough so that the liquid drains out of the foam (see calculations in Section S4), mechanism I (imbibition) stops completely since the foam does not gain energy by absorbing the oil (the bubbles at the bottom are already round). If the liquid fraction is high but liquid is retained in the foam, the effect is present but negligible. At higher liquid fractions ($\varepsilon \geq 15\%$), imbibition (mechanism I) no longer takes place, but drainage (mechanism III) instead plays a significant role in the cleaning. In order to show that drainage does not play a role for foams with low liquid fractions ($\varepsilon \leq 15\%$), we calculated the drainage profiles of our foams (see Section S4). Looking at the profiles (Figures S5 and S6), one sees that at the beginning of all experiments, drainage of liquid out of the foam is measurable only for foams with a liquid fraction of $\varepsilon = 20\%$. For foams without PFH, only foams with $\varepsilon = 15\%$ start to lose liquid towards the end of the experiment (see Figure S5, bottom). Thus, drainage of liquid out of the foam does not play a role for foams with $\varepsilon < 15\%$. The liquid drains out of the foam and flows under the dirt and lifts it from the surface. The dirt subsequently floats on the drained liquid. In the case of unstable PFH-free foam, wiping (mechanism II) additionally takes place, whereby both the soot particles and the oil are removed from the surface. However, in the case of the stable PFH-containing foam, no efficient cleaning effect can be seen (Figure 5). It seems that in the case without strong drainage, the soot particles interfere with the cleaning process. Thus, the oil and soot particles are not removed from the surface, as no additional wiping takes place in the stable foam. In

our study with only one dirt component (Schad et al., 2021), cleaning with the PFH-containing foam was most efficient at $\varepsilon = 20\%$. Moreover, at $\varepsilon = 20\%$, cleaning was similarly efficient both with and without PFH (Schad et al., 2021).

Therefore, cleaning is much more efficient with PFH-free foams, as in our previous study (Schad et al., 2021). As we expected from our previous study, cleaning with the PFH-free foams is much faster than with the PFH-containing foams independent of the liquid fraction. In order to take a closer look at imbibition and drainage, both processes were viewed from the side for stable and unstable foams ("Imbibition and drainage viewed from the side" section).

Imbibition and drainage viewed from the side

To analyze the imbibition and drainage process from the side, a glass cuvette was filled with colored sunflower oil and mixed with a spatula tip of soot particles (see "Model contaminated surfaces and experimental procedure" section). Afterward, the foams were deposited on top of the oil. Since imbibition takes place only at low liquid fractions, these tests were carried out with unstable PFH-free (Figure 6, top) and stable PFH-containing (Figure 6, bottom) foams with a liquid fraction of $\varepsilon = 5\%$. The photographs on the left of Figure 6 show the colored oil and the soot particles at the bottom of the glass cuvette. The photographs in the middle of Figure 6 show the cuvette 4 min after the foam was placed on the model contamination and a zoom on the imbibition.

The zoomed photograph of the PFH-free foam in the cuvette in Figure 6 (top, right) shows that both the colored oil and the soot particles are drawn into the foam. The soot particles are sucked into the foam together with the liquid by the suction on the liquid. In addition, the shear forces generated during wiping ensure that the particles are better detached from the surface, which improves cleaning by imbibition. Furthermore, the Plateau borders become larger because of the decay of the foam, making it easier for the soot particles to pass through.

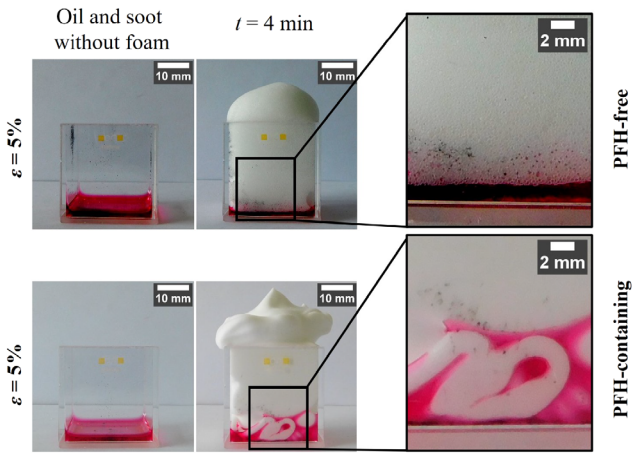

FIGURE 6 View of the imbibition process from the side. Photographs of the cuvettes with oil and soot without foam as well as 4 min after the application of the PFH-free (top) and the PFH-containing foam (bottom) with $\varepsilon = 5\%$

In the zoomed photograph 4 min after the application of the stable PFH-containing foam (Figure 6, bottom, right), the imbibition is hardly visible. One mainly sees how the oil and some soot particles move up the glass wall. However, imbibition takes place (see fig. 6 of Schad et al., 2021) but only with the oil, whereas the soot remains at the bottom of the cuvette. In our last study, we found that imbibition is slightly weaker in PFH-containing foams due to the smaller Plateau borders of the stable foam (Schad et al., 2021). It seems that the particles are simply too large to pass together with the oil through the very thin Plateau borders of the foam (see Section S3). In addition, there is no wiping with stable foam, which makes it more difficult to remove the particles from the surface. By comparing imbibition with and without PFH, it can be seen that imbibition takes place in both cases. However, with the PFH-containing foam, only the oil can be removed by imbibition while it is possible to remove both dirt components with the unstable PFH-free foam.

In addition to imbibition, the drainage of the foams from the side was also considered. Since drainage occurs at higher liquid contents (Schad et al., 2021), foams without (Figure 7, top) and with PFH (Figure 7, bottom) with a liquid fraction of $\varepsilon = 20\%$ were used for the experiment. The first photographs (Figure 7, left) show the cuvette with colored oil and soot at the bottom. In the following photographs, one sees the cuvette 4, 8, and 12 min after the foam was placed on the dirt components. In the cuvette with the PFH-free foam (Figure 7, top), the cleaning solution flows out of the foam with increasing time because of gravity (drainage). Both the colored oil and the soot particles are detached from the bottom of the cuvette and float on the drained cleaning solution.

The foam with PFH in the gas phase (Figure 7, bottom) simply sits on the contamination without any measurable drainage taking place. This is a natural consequence of the constant and very small bubble size, which ensures that the capillary forces of the foam are strong enough to maintain the liquid within the foam (Maestro et al., 2013). This is consistent with the results of the cleaning test (Figure 5, right), where almost no cleaning effect could be seen at a liquid fraction of 20%. Thus, measurable drainage takes place only in the case of unstable PFH-free foams, which contributes to cleaning at higher liquid fractions. The reason for a good cleaning effect while cleaning with the PFH-

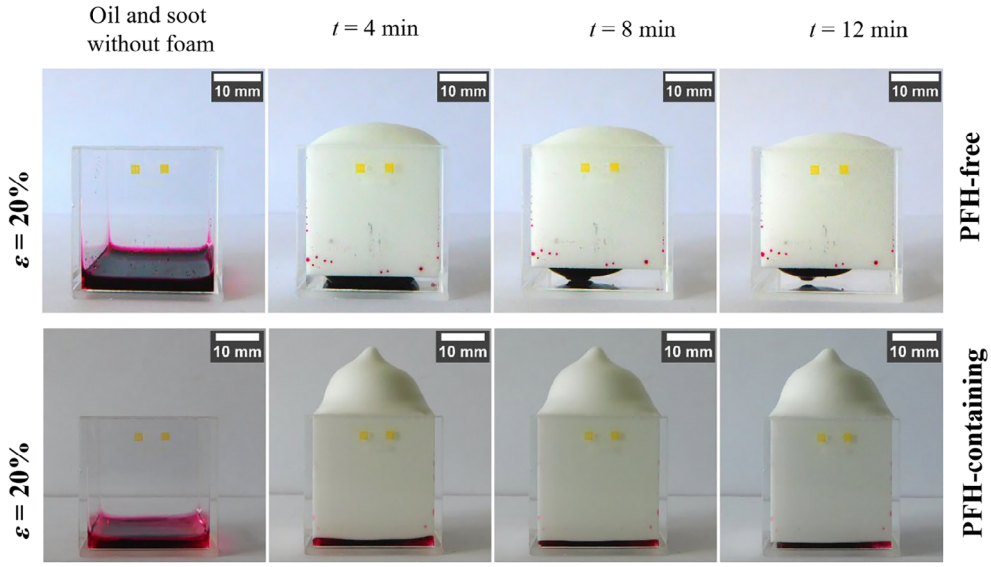

FIGURE 7 View of the drainage process from the side. Photographs of the cuvettes with oil and soot without foam as well as 4, 8, and 12 min after the application of the PFH-free (top) and PFH-containing foam (bottom) with $\varepsilon = 20\%$

containing foam with $\varepsilon = 20\%$ in the case of one contamination (oil) (Schad et al., 2021) and not in the case of both (oil and soot) is unexplained yet.

CONCLUSION

The current study complements our previous one (Schad et al., 2021) in which we carried out cleaning tests with foams with different liquid fractions and different stabilities. In the present study, we performed cleaning experiments with two instead of one model contamination, namely with colored sunflower oil and soot particles. On one hand, we varied the liquid fraction ε of the foams between 5% and 20%. On the other, we added perfluorohexane (PFH) to the gas phase in some cleaning experiments to generate foams with significantly higher stability. The foams were generated with the double-syringe technique: that is, the initial average bubble size was small (about $\langle r \rangle = 60\,\mu m$) and identical for all foams. The change of the contaminated area A_{dirt} on the glass plates was recorded with a digital camera during the cleaning with PFH-free and PFH-containing foams with different liquid fractions and subsequently analyzed. Like in our previous study, we found that cleaning with unstable PFH-free foams was much faster and more efficient compared to cleaning with stable PFH-containing foams at all liquid fractions. It was only after 15 min cleaning with PFH-free foams that a 60% decrease of A_{dirt} was observed at low liquid fractions ($\varepsilon \leq 10\%$) and an 80% decrease of A_{dirt} at higher liquid fractions ($\varepsilon \geq 15\%$). In contrast, with PFH-containing foams, less than 20% decrease of A_{dirt} was detected after 60 min.

We confirmed that the same three fundamental cleaning mechanisms as in our previous work (Schad et al., 2021) are involved in removing the two-component contamination from the glass plates: (i) imbibition takes place in cleaning with foams with low liquid fraction ($\varepsilon \leq 10\%$); (ii) drainage occurs at higher liquid fractions ($\varepsilon \geq 15\%$); and (iii) wiping plays an important role for unstable PFH-free foams. We showed that soot is removed from the contaminated surface by the oil entraining it. Wiping helps to detach both contaminations from the surface. Subsequently, the two-component contamination is sucked into the foam by imbibition (at low liquid fractions). However, an important difference is observed when the liquid channels of the foam (Plateau borders) are too small: the soot particles can no longer pass the Plateau borders and thus cleaning is less efficient.

As already mentioned, our aim is to develop a new foam-based cleaning method for sensitive historical surfaces which should not be exposed to the cleaning solution for long periods. For that purpose, unstable PFH-free foams with a low liquid fraction of $\varepsilon = 5\%$ (to reduce drainage) are the best choice. The next step is to systematically apply this cleaning approach to real historical objects. The first tests have already been successfully performed in Nymphenburg Palace in Munich. However, we need to significantly upscale the generation of foams with small bubbles and low liquid fractions for cleaning larger surfaces.

ACKNOWLEDGMENTS

We thank our cooperation partners Dr. Dirk Blunk, Universität zu Köln, and Dr. Heinrich Piening, Bayerische Verwaltung der staatlichen Schlösser, Gärten und Seen, Schloss Nymphenburg, with whom we work together on this project. We are grateful for the indispensable support of our mechanical (Daniel Relovsky) and electrical (Boris Tschertsche) workshops. We acknowledge funding from The German Federal Environmental Foundation (Deutsche Bundesstiftung Umwelt, DBU, AZ 34788/01-45) without

which this project would not have been feasible. Wiebke Drenckhan acknowledges additional financial support by an ERC consolidator grant (agreement 819511-METAFOAM), and Cosima Stubenrauch acknowledges a fellowship by the University of Strasbourg Institute for Advanced Studies (USIAS).

CONFLICT OF INTEREST

The authors declare that they have no conflict of interest.

ORCID

Cosima Stubenrauch https://orcid.org/0000-0002-1247-4006

REFERENCES

Andreev VA, Prausnitz JM, Radke CJ. Meniscus-shear particle detachment in foam-based cleaning of silicon wafers with an immersion/withdrawal cell. Ind Eng Chem Res. 2010;49:12461–70. https://doi.org/10.1021/ie1012954

Andreev VA, Freer EM, de Larios JM, Prausnitz JM, Radke CJ. Silicon-wafer cleaning with aqueous surfactant-stabilized gas/solids suspensions. J Electrochem Soc. 2010;158(1):H55–62. https://doi.org/10.1149/1.3503572

Andrieux S, Drenckhan W, Stubenrauch C. Generation of solid foams with controlled polydispersity using microfluidics. Langmuir. 2018;34:1581–90. https://doi.org/10.1021/acs.langmuir.7b03602

Baglioni P, Chelazzi D, Giorgi R, Poggi G. Colloid and materials science for the conservation of cultural heritage: cleaning, consolidation, and deacidification. Langmuir. 2013;29:5110–22. https://doi.org/10.1021/la304456n

Boos J, Drenckhan W, Stubenrauch C. On how surfactant depletion during foam generation influences foam properties. Langmuir. 2012;28:9303–10. https://doi.org/10.1021/la301140z

Chelazzi D, Giorgi R, Baglioni P. Microemulsions, micelles, and functional gels: how colloids and soft matter preserve works of art. Angew Chem Int Ed. 2018;57:7296–303. https://doi.org/10.1002/anie.201710711

Crowder GA, Taylor ZL, Reed TMK, Young JA. Vapor pressures and triple point temperatures for several pure fluorocarbons. J Chem Eng Data. 1967;12(4):481–5. https://doi.org/10.1021/je60035a005

Fournel B, Faure S, Pouvreau J, Dame C, Poulain S. Decontamination using foams: a brief review of 10 years French experience. Proceedings of 9th ASME international conference on radioactive waste management and environmental remediation, 2013; 37327:1483–9. https://doi.org/10.1115/ICEM2003-4526

Gaillard T, Roché M, Honorez C, Jumeau M, Balan A, Jedrzejczyk D, et al. Controlled foam generation using cyclic diphasic flows through a constriction. Int J Multiphase Flow. 2017;96:173–87. https://doi.org/10.1016/j.ijmultiphaseflow.2017.02.009

Gandolfo FG, Rosano H. Interbubble gas diffusion and the stability of foams journal of colloid. Interface Science. 1997;194:31–6. https://doi.org/10.1006/jcis.1997.5067

Höhler R, Yip Cheung Sang Y, Lorenceau E, Cohen-Addad S. Osmotic pressure and structures of monodisperse ordered foam. Langmuir. 2008;24:418–25. https://doi.org/10.1021/la702309h

Jones S, Rio E, Cazeneuve C, Nicolas-Morgantini L, Restagno F, Luengo GS. Tribological influence of a liquid meniscus in human sebum cleaning. Colloids Surf A Physicochem Eng Asp. 2016; 498:268–75. https://doi.org/10.1016/j.colsurfa.2016.03.047

Long CM, Nascarella MA, Valberg PA. Carbon black vs. black carbon and other airborne materials containing elemental carbon: physical and chemical distinctions. Environ Pollut. 2013;181:271–86. https://doi.org/10.1016/j.envpol.2013.06.009

Maestro A, Drenckhan W, Rio E, Höhler R. Liquid dispersions under gravity: volume fraction profile and osmotic pressure. Soft Matter. 2013;9:2531–40. https://doi.org/10.1039/C2SM27668B

Meagher AJ, Whyte D, Banhart J, Hutzler S, Weaire D, Garcia-Moreno F. Slow crystallisation of a monodisperse foam stabilised against coarsening. Soft Matter. 2015;11:4710–6. https://doi.org/10.1039/c4sm02412e

Mensire R, Lorenceau E. Stable oil-laden foams: formation and evolution. Adv Colloid Interface Sci. 2017;247:465–76. https://doi.org/10.1016/j.cis.2017.07.027

Mensire R, Piroird K, Lorenceau E. Capillary imbibition of aqueous foams by miscible and nonmiscible liquids. Phys Rev E. 2015; 92:05314. https://doi.org/10.1103/PhysRevE.92.053014

Mensire R, Ault JT, Lorenceau E, Stone HA. Point-source imbibition into dry aqueous foams. Europhys Lett. 2016;113:44002. https://doi.org/10.1209/0295-5075/113/44002

Schad T, Preisig N, Blunk D, Piening H, Drenckhan W, Stubenrauch C. Less is more: unstable foams clean better than stable foams. J Colloid Interface Sci. 2021;590:311–20. https://doi.org/10.1016/j.jcis.2021.01.048

Schneider CA, Rasband WS, Eliceiri KW. NIH image to ImageJ: 25 years of image analysis. Nat Methods. 2012;9:671–5. https://doi.org/10.1038/nmeth.2019

Steck K, Hamann M, Andrieux S, Muller P, Kéckicheff P, Stubenrauch C, et al. Fluorocarbon vapors suppress coalescence in foams, advanced materials. Interfaces. 2021;8: 2100723(1)–(6). https://doi.org/10.1002/admi.202100723

Weaire D, Pageron V. Frustrated froth: evolution of foam inhibited by aninsoluble gaseous component. Philos Mag Lett. 1990;62(6): 417–21. https://doi.org/10.1080/09500839008215544

SUPPORTING INFORMATION

Additional supporting information may be found in the online version of the article at the publisher's website.

How to cite this article: Schad T, Preisig N, Drenckhan W, Stubenrauch C. Foam-based cleaning of surfaces contaminated with mixtures of oil and soot. J Surfact Deterg. 2022;25: 377–85. https://doi.org/10.1002/jsde.12580

SUPPORTING INFORMATION

Foam-Based Cleaning of Surfaces Contaminated with Mixtures of Oil and Soot

Tamara Schad [1], Natalie Preisig [1], Wiebke Drenckhan [2], Cosima Stubenrauch,[1,3]*

[1] Universität Stuttgart, Institut für Physikalische Chemie, Pfaffenwaldring 55, 70569 Stuttgart, Germany

[2] Université de Strasbourg, CNRS, ICS UPR 22, F-67000 Strasbourg, France

[3] Institute of Advanced Studies (USIAS), University of Strasbourg, F-67000 France

*Corresponding Author: cosima.stubenrauch@ipc.uni-stuttgart.de, 0049 711 685-64470

S1. Editing of Photographs

The software *Fiji (Image J)* (Schneider et al., 2012) was used to analyze the recorded photographs. First, the photographs were cut to the same size. The scale of the photographs is 0.392 pixels / µm. The photographs were converted into black and white photographs using the three applications *Split Channels (red)*, *Adjust Brightness/Contrast* and *Adjust Threshold*. The *Analyze Particles* tool was used to calculate the contaminated area (black area (Fig. S1, IV) in the photographs. The contaminated area A_{dirt} is defined as 100% directly after the application of the foam. The photographs shown in this work are trimmed original photographs without editing. The software *Fiji* was also used to edit the photographs of the imbibition tests. First, the photographs were cut to the same size (*Crop*) and the contrast (*Adjust Brightness/Contrast*) was increased.

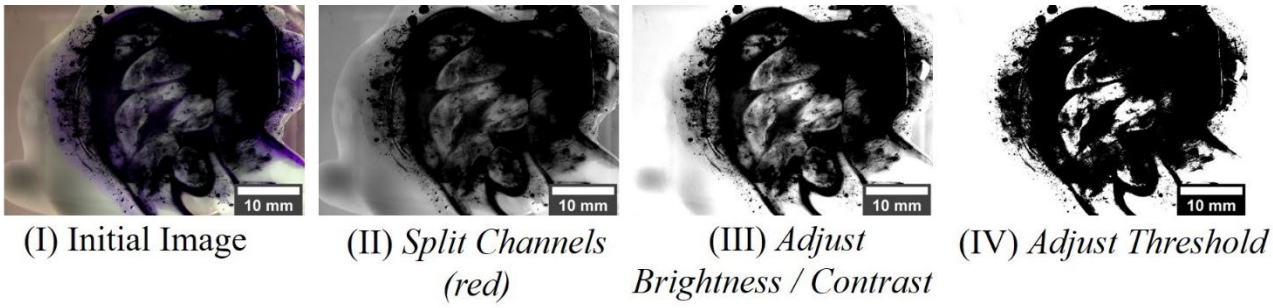

Fig. S1. Example of image processing using the image of the cleaning test with the PFH-containing foam with ε = 5 % at t = 0 min (I) with the consecutive steps: (II) *Split Channels (red)*, (III) *Adjust Brightness/Contrast* and (IV) *Threshold* to calculate the dirt area on the image using the *Analyze Particles* tool.

S2. Photographs of the cleaning tests

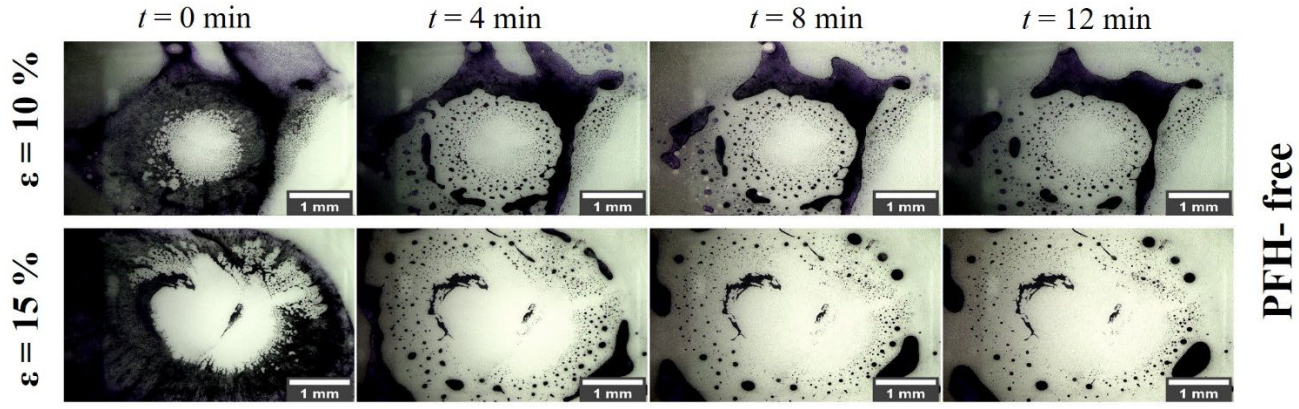

Fig. S2. Photographs of the cleaning tests from the bottom with PFH-free foams with different liquid fractions, namely ε = 10 % (top) and 15 % (bottom), right after application, after 4 min, 8 min, and 12 min.

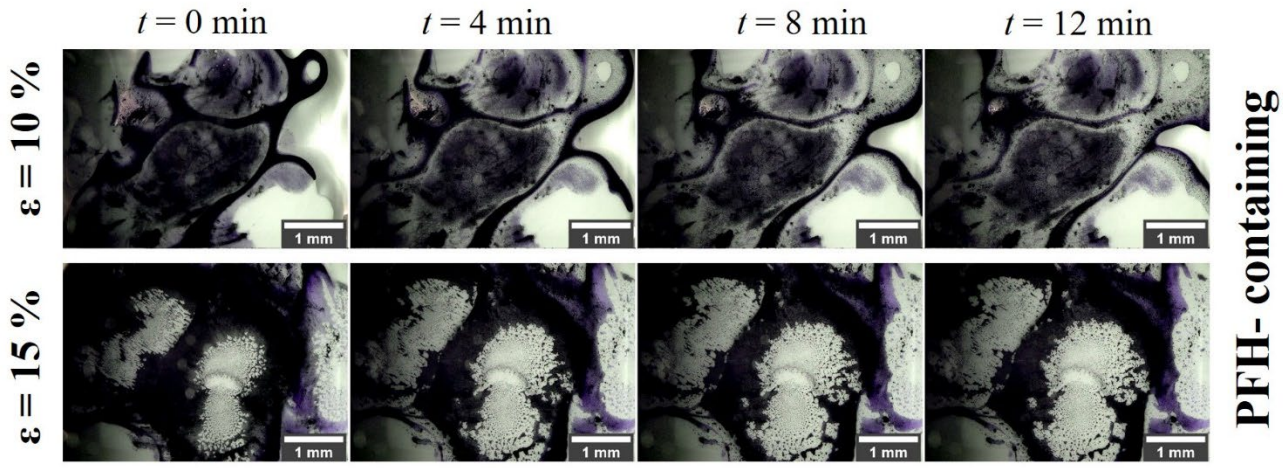

Fig. S3. Photographs of the cleaning tests from the bottom with PFH-containing foams with different liquid fractions, namely ε = 10 % (top) and 15 % (bottom) right after application, after 4 min, 8 min, and 12 min.

S3. Plateau Border Radii as Function of Bubble Size & Liquid Fraction

The size of the Plateau borders can be estimated with excellent accuracy assuming a Kelvin-type foam structure, for which the relationship between the bubble radius r, the Plateau border radius R and the liquid fraction ε is known (eq. (23) in (Drenckhan and Hutzler, 2015)). It holds

$$\varepsilon \sim 0.17(R/l)^2 + 0.2(R/l)^3$$

with

$$l = \left(\frac{\pi}{6\sqrt{2}}\right)^{1/3} r,$$

where l is the length of the Plateau borders. We plot this relationship for the three relevant scenarii of our experiments: (i) foams without PFH at the beginning of the experiment ($\langle r \rangle \approx 100$ µm), (ii) foams without PFH at the end of the experiment ($\langle r \rangle \approx 150$ µm), and (iii) foams with PFH during the entire experiment ($\langle r \rangle \approx 75$ µm). We can see that for the first two cases and for liquid fractions between 5 % ≤ ε ≤ 20 %, the Plateau border radii are between 50 µm and 130 µm. These radii are large enough for the soot particles (diameters of Ø = 30-160 µm) to pass, which is why there is an efficient removal of the particles with the PFH-free foams. However, in case of the PFH-containing foams, the Plateau border radii vary between 35-65 µm for 5 % ≤ ε ≤ 20 %, which obviously is too small for the soot particles too pass (and thus there is no efficient removal of the particles with the PFH-containing foams).

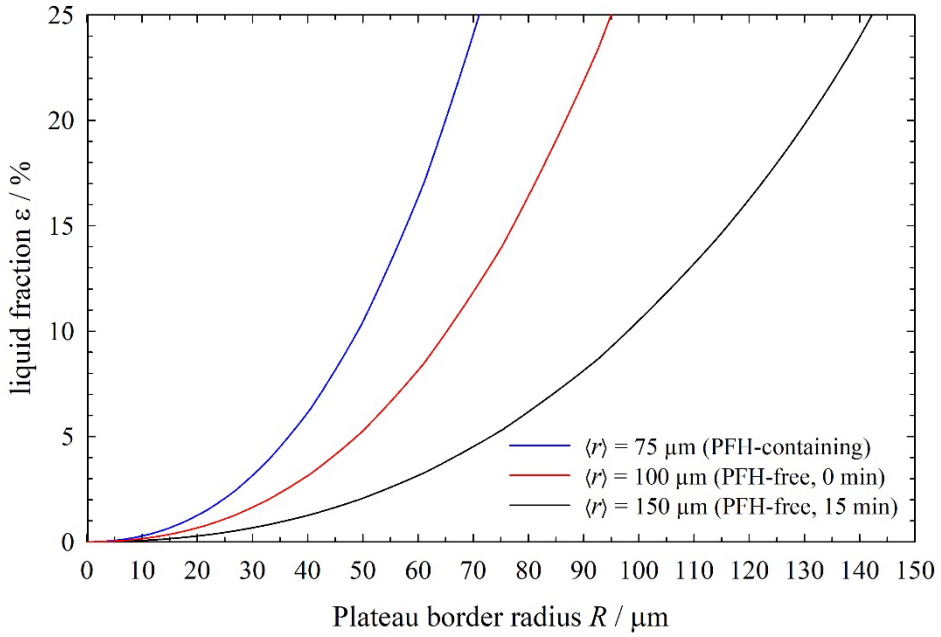

Figure S4: Relationship between liquid fraction ε and Plateau border radius R for three different bubble sizes $\langle r \rangle$: for PFH-free foams at the beginning ($\langle r \rangle$ = 100 µm) and at the end ($\langle r \rangle$ = 150 µm) of the experiment and for PFH-containing foams during the entire experiment ($\langle r \rangle$ = 75 µm).

S4. Drainage Profiles of Foams without and with PFH

Knowing the foam height (3.5 cm) and the bubble size, one can calculate the expected drainage profiles [eq. (8) in Maestro et al., 2013]. The resulting drainage profiles are shown in Figures S5 and S6. There are two possible scenarios. (1) If the two areas S_1 and S_2 (see Figure S5, top right) between the vertical grey line and the colored drainage curve are equal, the liquid that drains out of the upper part of the foam is collected in the lower part of the foam. In this case, the liquid is redistributed in the foam but it does not leave the foam, *i.e.* it does not drain out of the foam. (2) If the left area S_1 between the vertical grey line and the colored drainage curve is larger than the right one (S_2), the liquid that drains out of the upper part of the foam is only partly collected in the lower part of the foam. In this case, the liquid leaves the foam, *i.e.* it drains out of the foam. Looking at Figures S5 and S6, one sees that at the beginning of all experiments, drainage of liquid out of the foam is measurable only for foams with a liquid fraction of ε = 20%. For foams without PFH, only the foam with ε = 15% starts to lose liquid towards the end of the experiment (Figure S5 (bottom)). Hence, we can safely assume that another effect than drainage must play the key role for the foams with low liquid fractions.

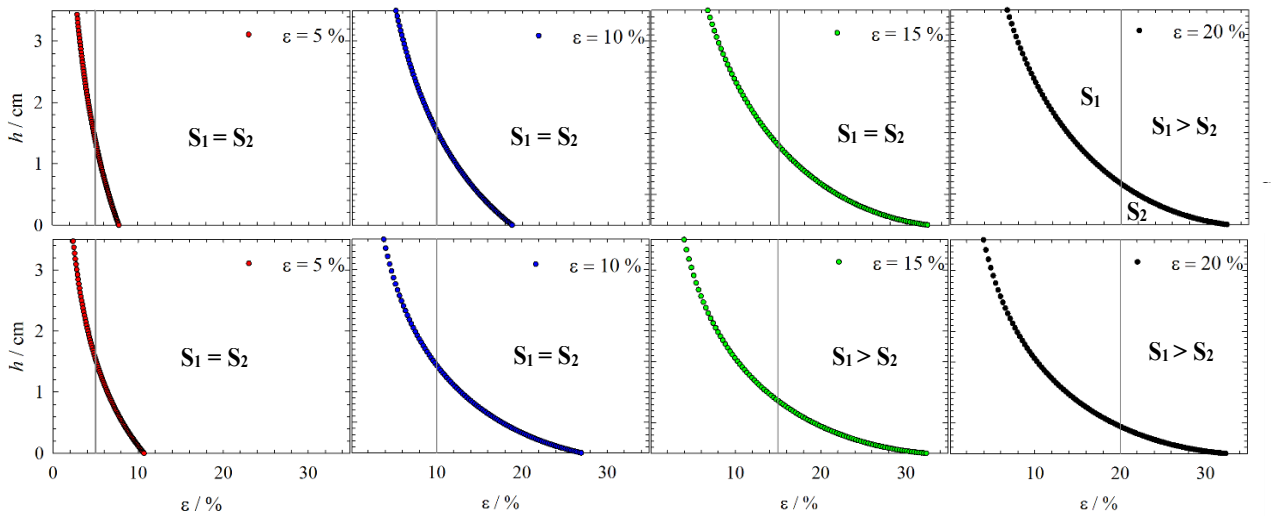

Figure S5: Equilibrium drainage profiles (cycles) calculated for PFH-free foams (foam height h = 3.5 cm) with the mean bubble size (top) $\langle r \rangle$ = 100 µm (at the beginning of the experiment) and (bottom) $\langle r \rangle$ = 150 µm (at the end of the experiment) at different liquid fractions ε. The solid lines show the initial liquid fraction ε.

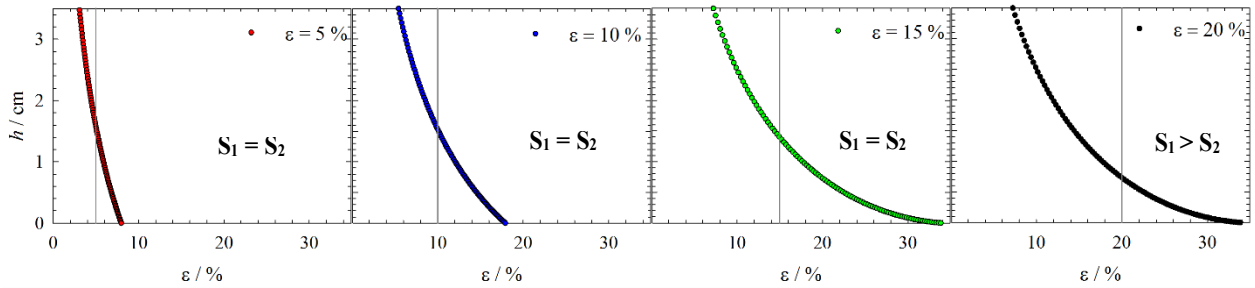

Figure S6: Equilibrium drainage profiles (cycles) calculated for PFH-containing foams (foam height h = 3.5 cm) with the mean bubble size $\langle r \rangle$ = 75 µm (during the entire experiment) at different liquid fractions ε. The solid lines show the initial liquid fraction ε.

References

Drenckhan W., Hutzler S., Structure and energy of liquid foams, Advances in Colloid and Interface Science, 2015, 224:1–16, doi: 10.1016/j.cis.2015.05.004

Maestro A., Drenckhan W., Rio E., Höhler R., Liquid dispersions under gravity: volume fraction profile and osmotic pressure, Soft Matter, 2013; 9:2531-2540. doi:10.1039/C2SM27668B

Schneider CA, Rasband WS, Eliceiri KW. NIH image to ImageJ: 25 years of image analysis. Nat Methods. 2012;9:671–675. https://doi.org/10.1038/nmeth.2019